*Korean J. Chem. Eng.*, 34(9), 2502-2506 (2017)
DOI: 10.1007/s11814-017-0142-x

pISSN: 0256-1115
eISSN: 1975-7220

# Effects of oxygen plasma generated in magnetron sputtering of ruthenium oxide on pentacene thin film transistors

**Taehyung Lee*,‡, Boram Lim**,‡, Kijung Yong*, Woosung Kwon**,†, and Minwoo Park**,†**

*Department of Chemical Engineering, Pohang University of Science and Technology (POSTECH),
77 Cheongam-ro, Pohang 37673, Korea
**Department of Chemical and Biological Engineering, Sookmyung Women's University,
100 Cheongpa-ro 47-gil, Seoul 04310, Korea
(*Received 19 March 2017 • accepted 21 May 2017*)

**Abstract**−Effects of oxygen plasma generated in a sputtering process for deposition of electrodes on pentacene thin films to configure top-contact (TC) transistors have been thoroughly investigated. Reactive oxygen species severely degraded electrical properties of pentacene films during the deposition of $RuO_x$ electrodes, leading to a failure of devices. In the off-region, the leakage current increased by about two orders of magnitude, and the subthreshold slope also increased by 6.5 times. The top surface of pentacene films was oxidized by oxygen plasma and C-O and C=O bonds awerere created. The pentacenequinone derivative was confirmed by X-ray photoelectron spectroscopy. The oxidation of pentacene films gives rise to charge traps at the pentacene/electrode interface, which produces a leakage channel between source and drain electrodes. We believe that this side effect of oxygen plasma on the fabrication of TC-devices should be considered carefully.

Keywords: Pentacene, Thin-film Transistor, Ruthenium Oxide, Oxygen, Plasma

## INTRODUCTION

Numerous studies on organic semiconductors for several decades have contributed immensely to development of the mobile and display industry. Outstanding luminescent efficiency and mechanical flexibility of this class of materials have been utilized for large-area and flexible organic light-emitting diodes (OLEDs) [1]. Meanwhile, they have been still undesirable for electronic devices requiring high switching speeds due to their inferior charge carrier mobility than conventional inorganic semiconductors such as GaAs and Si. As such, many efforts to enhance the performance of organic thin films transistors (OTFTs) have been made with two perspectives: Improvement of electrical properties of organic semiconductors and optimization of device architecture. For the latter, the deposition order of components (e.g., semiconductors and electrodes) would be crucial since it produces different results of device performance [2-7]. More specifically, two-device structures have been employed in OTFTs, a bottom and a top contact. It has been well known that top-contact (TC) devices show better performance than bottom-contact (BC) devices, since low contact resistance between source/drain (S/D) electrodes and a semiconductor layer allows less electron-scattering at the interface [8]. Moreover, band alignment of the electrodes and semiconductor layers has become the key to attaining high device performance. For example, $NiO_x$ and $RuO_x$ prepared by sputtering process have more suitable work function ($\Phi$) than pure metals for *p*-type organic semiconductors. In a BC-pentacene TFTs, the higher field-effect mobility and on/off ratio were observed when $NiO_x$ and $RuO_x$ ($\Phi$=5.0 eV and 4.92 eV, respectively) were used, which was attributed to the more efficient hole injection from the highest occupied molecular orbital (HOMO, 5.1 eV) of pentacene to the metal electrodes than when Ni ($\Phi$=4.6 eV), Ru ($\Phi$=4.64 eV) and even Au ($\Phi$=4.85 eV) were used for electrodes [9-11]. However, the effect of such metal oxides on organic semiconductor layers and device performance during the deposition has not been reported for TC-devices.

Herein, we report on the effect of radio frequency (RF) magnetron sputtering of $RuO_x$ on pentacene thin films. After deposition of $RuO_x$, the oxidized pentacene, 6,13-pentacenequinone, is observed on the top surface of the pentacene film by X-ray photoelectron spectroscopy (XPS) analysis. Even though field-effect mobility of the devices is improved from 0.308 $cm^2/V\cdot s$ to 0.499 $cm^2/V\cdot s$ as the flow rate of oxygen gas increases, the high charge trap density at the pentacene/$RuO_x$ interface leads to the high level of leakage currents and significant drop in the on/off ratio.

## EXPERIMENTAL DETAILS

$SiO_2$ (300 nm)/N++Si substrates (Silicon Material Inc.) were immersed into 7 : 4 (volume ratio) $H_2SO_4/H_2O_2$ solution (piranha solution) at 100 °C for 1h to remove organic residues, and cleaned in an UV tip-cleaner (UV TC 220, Pucotech) for 1 hr. To provide good surface coverage of pentacene on $SiO_2$, octadecyltrichlorosilane self-assembled monolayers (OTS-SAM) were deposited on the $SiO_2$ by immersing the substrates for 6 h at 4 °C into an anhydrous toluene (99.8%, Aldrich) solution containing 10 mmol of OTS (Aldrich)

†To whom correspondence should be addressed.
E-mail: wkwon@sm.ac.kr, mwpark@sm.ac.kr
‡These authors contributed equally to this work.
Copyright by The Korean Institute of Chemical Engineers.

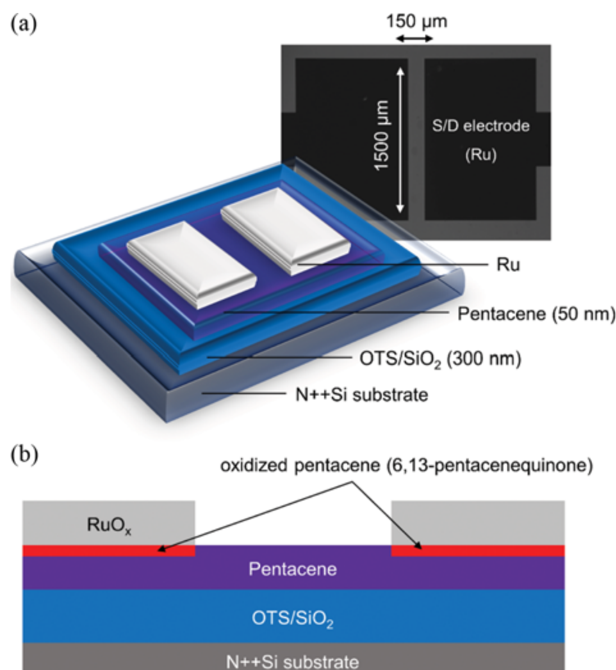


**Fig. 1. Schematic illustrating (a) the pentacene TFT with a 150 μm-long and 1,500 μm-wide channel and (b) the leakage channel (indicated by the red squares) formed at the pentacene/electrode interface.**

[12]. The substrates treated with SAM were further cleaned in acetone, and annealed in a vacuum chamber for 2 h at 150 °C. 50 nm-thick pentacene thin films were deposited in an organic molecular beam deposition (OMBD) reactor at 70 °C and $2\times10^{-6}$ Torr with a deposition rate of 0.2-0.3 Å/sec. A shadow mask was used during the deposition to pattern the pentacene layer. The Ru and $RuO_x$ S/D electrodes were deposited with RF magnetron sputtering under the argon and oxygen atmosphere, respectively. The deposition was at a working pressure of 7 mTorr with the RF power of 50 W. The composition of the sputtering atmosphere was controlled by controlling the flow rate of argon and oxygen. The channel dimension had a length of 150 μm and a width of 1,500 μm as shown in Fig. 1(a). The I-V characteristics of the device were measured with an Agilent E5270A precision semiconductor parameter analyzer. Oxidation of pentacene thin films was by using an UV tip-cleaner with different exposure times (30, 60, 120 and 180 min). The surface morphology of pentacene was investigated with an atomic force microscope (AFM, Veeco Dim. V). The variations in the molecular structure of pentacene were observed with a X-ray photoelectron spectroscope (XPS, the 4B1 beam line in the Pohang Acceleration Laboratory synchrotron radiation source).

## RESULTS AND DISCUSSION

Fig. 1(a) (top view) and1B (side view) exhibit the schematic of the TC-pentacene TFT. When $RuO_x$ electrodes were deposited in the presence of oxygen plasma, highly reactive oxygen species could react with the pentacene film [13]. As shown in Fig. 1(b), such reaction has an effect right on the top surface of the pentacene film, and pentacenequinone derivatives are formed. To elucidate the effect of oxygen plasma damage, the performance of both BC- and TC-devices, and the surface morphologies of pentacene should be investigated.

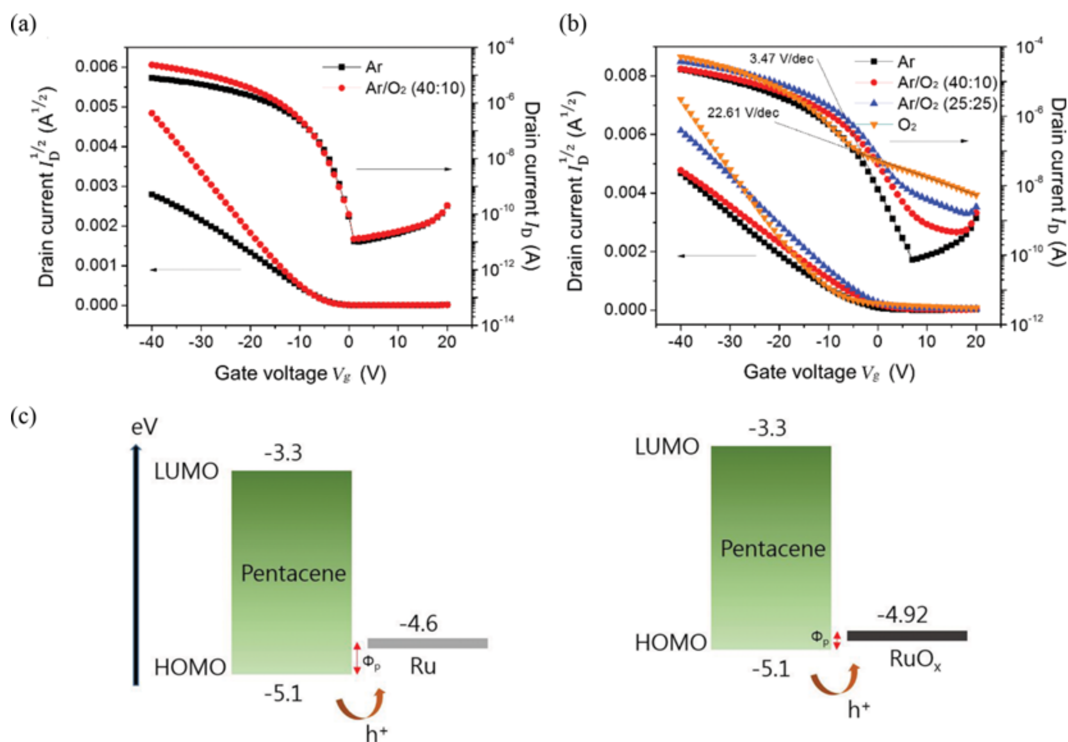


**Fig. 2. Saturation transfer curves of the (a) BC- and (b) TC-devices. (c) Schematic illustrating energy diagram of pentacene, Ru and $RuO_x$.**

Fig. 2(a) and 2(b) show the typical field-effect transfer curves of the BC- and TC-device, respectively. No effects by oxygen plasma were observed in the devices since Ru sputtering preceded the deposition of pentacene at the BC-devices. As the flow rate of oxygen gas increased, the performance of BC-devices was improved with the retention of subthreshold voltage swings and off-currents (Fig. 2(a)). The subthreshold slope, S, is defined as

$$S=\frac{dV_G}{d\log I_D} \tag{1}$$

where $V_g$ is the gate voltage and $I_D$ is the drain current. The S value is proportional to the areal density of interfacial traps ($N_{trap}$) at the pentacene/electrode interface as shown below [14,15],

$$N_{trap}\cong\left[\frac{qS\log(e)}{kT}-1\right]\frac{C_{ox}}{q} \tag{2}$$

where q is the electronic charge, k is the Boltzmann constant, and $C_{ox}$ is the dielectric capacitance per unit area. S was found to be 1.32 V/decade and 1.43 V/decade for the BC-Ru and $RuO_x$ device, respectively. Therefore, $N_{trap}$ of both devices was similar to each other because it was proportional to the S value. And no effect on the threshold voltages ($V_{th}$) was observed, 4.84 V and 4.77 V for BC-Ru and $RuO_x$ device, respectively. The off-current in the BC-$RuO_x$ device was found to be $1.28\times10^{-11}$ A, which was comparable to the value ($1.00\times10^{-11}$ A) of the Ru device.

The field-effect mobility ($\mu$) is expressed by the slope at the saturated regime on the bottom curves,

$$I_D=\frac{WC_{ox}}{2L}(V_g-V_{th})^2\mu \tag{3}$$

where W is the channel width, $V_g$ is the gate voltage and L is the channel length. From the above equation, $\mu$=0.205 $cm^2/V\cdot s$ and 0.435 $cm^2/V\cdot s$ for the BC-Ru device and $RuO_x$ device, respectively. In addition to the mobility, on/off ratio was also enhanced from $7.53\times10^5$ to $1.83\times10^6$.

Meanwhile, top-contact (TC) devices showed dramatic degradation of the device performance when pentacene was exposed to oxygen plasma. Fig. 2(b) clearly indicates the effect of the flow rate of oxygen gas on the I-V characteristics in the TC-devices. In the absence of oxygen, the field-effect characteristics of TC-Ru device were found that $\mu$=0.308 $cm^2/V\cdot s$, on/off ratio=$2.92\times10^5$ and off-current=$7.50\times10^{-11}$ A. An upward shift of the transfer curves at off-regions was observed as the flow rate of oxygen gas increased, which indicated that the flow of leakage currents became more dominant. At $Ar:O_2$=40 : 10, the off-current and subthreshold swing dramatically increased to $4.66\times10^{-10}$ and 14.29 V/decade, respectively; this was attributed to the increasing trap sites at the pentacene/electrode interface. At above $Ar:O_2$=25 : 25, the function of OTFTs lost because on/off ratio was not determined. The top surface of the pentacene layer was severely damaged, thereby the leakage path became comparable to the intrinsic channel and the device eventually broke down. But the field-effect mobility of TC-devices still increased up to 0.499 $cm^2/V\cdot s$ since the suitable work function of $RuO_x$ to HOMO of pentacene allowed the reduction of hole injection barrier ($\phi_p$), as shown in the BC-$RuO_x$ device with similar tendency. In Fig. 2(c), $\phi_p$ at the pentacene/$RuO_x$ interface is lower than that at the pentacene/Ru interface. Recently, Hwang et al. reported that increase in the oxygen content (or oxygen deficiency level) during sputtering deposition slightly increased work function of $RuO_x$ on $SiO_2$ from 5.29 eV to 5.37 eV at 10.4% and 14.3%, respectively [16]. Therefore, the efficient hole injection from pentacene in the $RuO_x$ devices led to the high field-effect mobility both BC- and TC-$RuO_x$ devices. The several parameters of field-effect characteristics in BC- and TC-devices are summarized in Table 1 and Table 2, respectively.

It is well known that oxygen plasma strongly degrades conducting polymers and small molecules [17-19]. The atomic bonds in their functional group (i.e., thiophene and acene rings), which contains high carrier density, are easily broken by reactive oxygen species and ultraviolet (UV) light. The broken sites make a new bond with oxygen or hydroxyl groups and they trap the charge carriers, which leads to the degradation of device performance including a field-effect mobility, an on/off ratio and a sub-threshold characteristics [18,19]. Therefore, an in-depth analysis of variation in molecular structure and surface morphology of pentacene layers should be performed after they are exposed to oxygen plasma.

The XPS analysis in Fig. 3 clearly exhibits the changes in the molecular structure of pentacene after it was exposed to oxygen

**Table 1. Field-effect properties of the BC-devices varying with the flow rate of the oxygen gas**

| BC electrodes ($Ar:O_2$) | Off current (A) | Subthreshold slope (V/decade) | Threshold voltage (V) | Field-effect mobility ($cm^2/V\cdot s$) | On/off ratio |
|---|---|---|---|---|---|
| Ru | $1.00\times10^{-11}$ | 1.32 | 4.84 | 0.205 | $7.53\times10^5$ |
| $RuO_x$ (40 : 10) | $1.28\times10^{-11}$ | 1.43 | 4.77 | 0.435 | $1.83\times10^6$ |

**Table 2. Field-effect properties of the TC-devices varying with the flow rate of the oxygen gas**

| TC electrodes ($Ar:O_2$) | Off current (A) | Subthreshold slope (V/decade) | Threshold voltage (V) | Field-effect mobility ($cm^2/V\cdot s$) | On/off ratio |
|---|---|---|---|---|---|
| Ru | $7.50\times10^{-11}$ | 3.47 | 4.86 | 0.308 | $2.92\times10^5$ |
| $RuO_x$ (40 : 10) | $4.66\times10^{-10}$ | 14.29 | 8.43 | 0.319 | $9.59\times10^3$ |
| $RuO_x$ (25 : 25) | $1.59\times10^{-9}$ | 18.84 | 9.39 | 0.499 | - |
| $RuO_2$ (0 : 50) | $5.40\times10^{-9}$ | 22.61 | - | - | - |

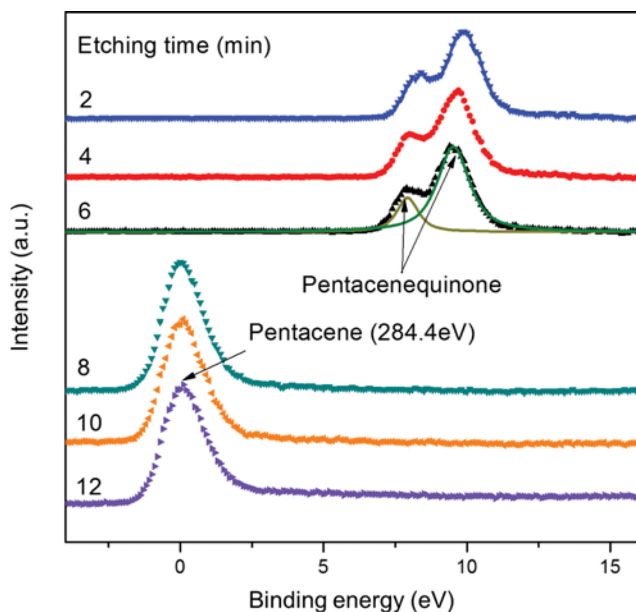


**Fig. 3. C1s XPS spectra (depth profile) of the 50 nm-thick pentacene film exposed to the oxygen plasma for 30 s.**

plasma for 30 s. During Ar etching of a 50 nm-thick pentacene thin film (etching rate=1 nm/min), the characteristic peaks of 6, 13-pentacenequinone were observed until 6 min. It was confirmed by the emergence of two peaks from single peak (284.4 eV) at the C1s core level corresponding to 284.9 eV and 287.3 eV, respectively [20, 21]. The peaks disappeared after further etching of the thin film (etching time>8 min). That is, about 6 nm-thick 6, 13-pentacenequinone layer was created from the outermost surface of pentacene. This demonstrated that the generation of C=O and C-O bonds in 6, 13-pentacenequinone by oxidation resulted in the charge trapping at the interface with electrodes, which produced the high level of leakage currents at the interface, not at the bottom layer of pentacene contacted to $SiO_2$.

We also investigated the morphological changes in the pentacene films by using AFM. Fig. 4 shows the AFM images obtained after oxygen plasma and ultraviolet (UV) light treatment to the films with different exposure times (0-180 min). In addition to oxygen plasma, UV light also generates highly reactive oxygen radicals in air and they oxidize organic materials [22-24]. The pentacene grains (200-500 nm) were easily decomposed and evaporated at room temperature, since 6, 13-pentacenequinone consisted of an intermediate phase, and it was volatile as well [25]. The fast degradation speed under oxygen plasma treatment was attributed to the fact that higher power of oxygen plasma (50 W) than that of UV light (20 W) produced a higher level of oxygen radicals. From these results, it should be considered that the sputtering process to deposit metal oxide-electrodes results in severe damage to an organic semiconductor at the configuration of TC-devices.

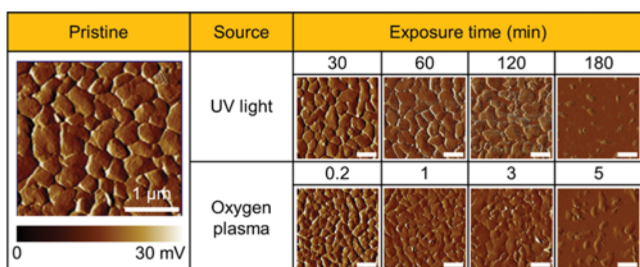


**Fig. 4. AFM images (5 μm×5 μm) of the 50 nm-thick pentacene films obtained by tapping mode. The samples were exposed to UV light and oxygen plasma for different exposure times. The scale bars are 500 nm.**

## CONCLUSIONS

We observed that RF magnetron sputtering of Ru damaged pentacene thin films and degraded their electrical properties. The oxidation of the pentacene film by oxygen plasma gave rise to many charge traps at the pentacene/electrode interface. As the result, the subthreshold slopes and leakage currents in the TC-$RuO_x$ devices significantly increased, whereas the performance of BC-$RuO_2$ devices was superior to that of BC-Ru devices. From the XPS analysis, the oxidized pentacene film exhibited a significant positive shift of binding energy due to its high oxidation level, which turned out to be 6, 13-pentacenequinone derivatives. The AFM images showed that pentacene films were readily decomposed in the presence of both oxygen plasma and UV light. These results suggest that the chemical damage to organic semiconductors by the reactive gas species should be considered when TC-OTFTs are fabricated.

## ACKNOWLEDGEMENT

This research was supported by the Basic Science Research Programs of the National Research Foundation (NRF) of Korea funded by the Ministry of Science, ICT & Future Planning (2016R1C1B1011830 and 2016R1C1B2011016). W.K. is grateful to Hyun-Jin Park (NINT, Pohang, South Korea) for his assistance in the atomic force microscopy.

## REFERENCES

1. K. T. Kamtekar, A. P. Monkman and M. R. Bryce, *Adv. Mater.*, **22**, 572 (2010).
2. C. R. Newman, C. D. Frisbie, D. A. da Silva Filho, J.-L. Bredas, P. C. Ewbank and K. R. Mann, *Chem. Mater.*, **16**, 4436 (2004).
3. E. Fortunato, P. Barquinha and R. Martins, *Adv. Mater.*, **24**, 2945 (2012).
4. A. R. Murphy and J. M. J. Frechet, *Chem. Rev.*, **107**, 1066 (2007).
5. S. W. Rhee and D. J. Yun, *J. Mater. Chem.*, **18**, 5437 (2008).
6. A. Facchetti, M. H. Yoon and T. J. Marks, *Adv. Mater.*, **17**, 1705 (2005).
7. C. D. Dimitrakopoulos and P. R. L. Malenfant, *Adv. Mater.*, **14**, 99 (2002).
8. P. Cosseddu and A. Bonfiglio, *Thin Solid Films*, **515**, 7551 (2007).
9. D. J. Yun, S. Lee, K. Yong and S.-W. Rhee, *Appl. Phys. Lett.*, **97**, 073303 (2010).
10. D. J. Yun and S. W. Rhee, *J. Electrochem. Soc.*, **155**, H899 (2008).
11. C. W. Chu, S. H. Li, C. W. Chem, V. Shrotriya and Y. Yang, *Appl. Phys. Lett.*, **87**, 193508 (2005).

12. X.-H. Zhang, B. Domercq, X. Wang, S. Yoo, T. Kondo, Z. L. Wang and B. Kippelen, *Org. Electron.*, **8**, 718 (2007).
13. D. H. Kim, D. W. Kim, K. S. Kim, H. J. Kim, J. S. Moon, M. P. Hong, B. S. Kim, J. H. Shin, Y. M. Kim, K. K. Song and S. S. Shin, *Jpn. J. Appl. Phys.*, **47**, 5672 (2008).
14. A. Rolland, J. Richard, J.-P. Kleider and D. Mencaraglia, *J. Electrochem. Soc.*, **140**, 3679 (1993).
15. M. McDowell and I. G. Hill, *Appl. Phys. Lett.*, **88**, 073505 (2006).
16. H. K. Kim, I.-H. Yu, J. H. Lee, T. J. Park and C. S. Hwang, *ACS Appl. Mater. Interfaces*, **5**, 1327 (2013).
17. S. Park, W. Kim and Y. Kim, *Korean J. Chem. Eng.*, **34**, 1500 (2017).
18. F. So and D. Kondakov, *Adv. Mater.*, **22**, 3762 (2010).
19. M. Park, J.-S. Park, I. K. Han and J. Y. Oh, *J. Mater. Chem. A.*, **4**, 11307 (2016).
20. S. J. Kang, Y. Yi, C. Y. Kim, K.-H. Yoo, A. Moewes, M. H. Cho, J. D. Denlinger, C. N. Whang and G. S. Chang, *Phys. Rev. B*, **72**, 205328 (2005).
21. P. Parisse, S. Picozzi and L. Ottaviano, *Org. Elec.*, **8**, 498 (2007).
22. H. W. Zan and C.-W. Chou, *Jpn. J. Appl. Phys.*, **48**, 031501 (2009).
23. K. Ono, H. Totani, T. Hiei, A. Yoshino, K. Saito, K. Eguchi, M. Tomura, J. Nishida and Y. Yamashita, *Tetrahedron*, **63**, 9699 (2007).
24. Y. Matsumoto, T. Ohsawa, K. Nakajima and H. Koinuma, *Meas. Sci. Technol.*, **16**, 199 (2005).
25. A. Vollmer, H. Weiss, S. Rentenberger, I. Salzmann, J. P. Rabe and N. Koch, *Surf. Sci.*, **600**, 4004 (2006).